

# Homogenization approach to filtration through a fibrous medium

Mohamed Belhadj, Eric Cancès, Jean-Frédéric Gerbeau, Andro Mikelic

► **To cite this version:**

Mohamed Belhadj, Eric Cancès, Jean-Frédéric Gerbeau, Andro Mikelic. Homogenization approach to filtration through a fibrous medium. [Research Report] RR-5277, INRIA. 2004. inria-00071254

**HAL Id: inria-00071254**

**<https://hal.inria.fr/inria-00071254>**

Submitted on 23 May 2006

**HAL** is a multi-disciplinary open access archive for the deposit and dissemination of scientific research documents, whether they are published or not. The documents may come from teaching and research institutions in France or abroad, or from public or private research centers.

L'archive ouverte pluridisciplinaire **HAL**, est destinée au dépôt et à la diffusion de documents scientifiques de niveau recherche, publiés ou non, émanant des établissements d'enseignement et de recherche français ou étrangers, des laboratoires publics ou privés.

# *Homogenization approach to filtration through a fibrous medium*

Mohamed Belhadj — Eric Cancès — Jean-Frédéric Gerbeau — Andro Mikelić

**N° 5277**

Juillet 2004

Thèmes NUM et BIO



*Rapport  
de recherche*



## Homogenization approach to filtration through a fibrous medium

Mohamed Belhadj <sup>\*</sup>, Eric Cancès <sup>† ‡</sup>, Jean-Frédéric Gerbeau <sup>§</sup>, Andro Mikelić <sup>¶</sup>

Thèmes NUM et BIO — Systèmes numériques et Systèmes biologiques  
Projets BANG, MICMAC et REO

Rapport de recherche n° 5277 — Juillet 2004 — 28 pages

**Abstract:** We study the flow through fibrous media using homogenization techniques. The fiber network under study is the one already used by M. Briane in the context of heat conduction of biological tissues. We derive and justify the effective Darcy equation and the permeability tensor for such fibrous media. The theoretical results on the permeability are illustrated by some numerical simulations. Finally, the low solid fraction limit is considered. Applying results by G. Allaire to our setting, we justify rigorously the leading order term in the empirical formulas for the effective permeability used in engineering. The results are also confirmed by a direct numerical calculation of the permeability, in which the small diameter of the fibers requires high accuracy approximations.

**Key-words:** Homogenization, Filtration, Fibrous Porous Media, Quasi-periodic, Darcy Equation, Permeability, Low Solid Fraction.

\* INRIA Rocquencourt - Projet BANG

† Ecole Nationale des Ponts et Chaussées-CERMICS

‡ INRIA Rocquencourt - Projet MICMAC

§ INRIA Rocquencourt - Projet REO

¶ Université Lyon 1 - LaPCS, UFR Mathématiques

## **Approche par homogénéisation de la filtration à travers un milieu fibreux**

**Résumé :** Nous étudions, par des techniques de l'homogénéisation, la filtration au travers de milieux poreux fibrés. Le réseau des fibres étudié est celui utilisé par M. Briane dans le cadre d'une étude sur la conduction thermique des tissus biologiques. Nous dérivons et justifions l'équation de Darcy ainsi que la forme du tenseur de perméabilité pour un tel milieu fibreux. Les résultats théoriques concernant la perméabilité sont illustrés par quelques simulations numériques. Finalement, nous considérons le cas où le diamètre des fibres tend vers zéro. En appliquant des résultats de G. Allaire à notre cas, nous justifions rigoureusement la forme du terme dominant dans les formules de perméabilité efficace utilisées en ingénierie. Ces résultats sont également confirmés par un calcul numérique direct de la perméabilité, dans lequel la petitesse du diamètre des fibres rend nécessaire le recours à des approximations de précision élevée.

**Mots-clés :** Homogénéisation, Filtration, Milieu Poreux Fibré, Quasi-périodique, Equation de Darcy, Perméabilité, Faible Fraction Solide.

## 1 Introduction

Filtration through fibrous porous media is of considerable interest in various engineering systems. Common examples of fibrous media include industrial filters, biological tissues, certain polymer membranes and many materials produced in the paper industry.

In most applications, flow in porous media is modelled by using a generalized form of Darcy's law:

$$\mathbf{u} = -\frac{\mathbf{K}}{\nu} \nabla p, \quad (1)$$

where  $\mathbf{u}$  is the filtration velocity,  $p$  denotes the fluid pressure,  $\nu$  is the fluid viscosity and  $\mathbf{K}$  stands for the permeability tensor of the porous material.

Darcy equations can be derived by means of homogenization techniques starting from the Stokes flow through an array of particles.

Ene and Sanchez-Palencia seem to be first to give a derivation of it, from the Stokes system, using a formal multiscale expansion (see [16]). This derivation was made rigorous in the case of a  $2D$  periodic porous medium by L. Tartar in [43]. This result was generalized in number of other papers. We mention the generalization to  $3D$  by G. Allaire [2] and to a random statistically homogeneous porous medium by Beliaev and Kozlov [9].

The knowledge of the permeability which expresses the flow resistance of a fibrous porous medium is an important matter in the design of industrial filters and artificial porous media. Hence many works have been conducted to study the permeability of different fibre distributions in the medium. These works can be divided into pure experimental ones, pure theoretical ones, and works based on an analytical approach with elements of computational methods for the determination of permeability. A comprehensive review of the literature on permeability of fibrous media has been elaborated by Jackson and James [24]. These authors discuss a variety of theoretical models and present a large collection of experimental data for both natural and synthetic fibrous media. Predominantly, these models use two-dimensional representations of fibrous media, and consider both parallel and transverse flow through spatially periodic arrays of cylinders (for a detailed discussion we refer for example to [15, 19, 31, 32, 38, 41]).

For two-dimensional sparse media, Howells [21] developed a theory for dilute random arrays of parallel cylinders using an averaged-equation approach. Sangani and Yao [39, 40] conducted numerical simulations of random arrays of parallel cylinders, finding good agreement with the predictions of Howells at low concentrations.

While there is a large literature on two-dimensional models, relatively few papers have been written that address three-dimensional, fibrous porous media.

For three-dimensional media, there are two studies cited by Jackson and James (see [23, 42]). In [20], Higdon and Ford use a rigorous numerical technique, the spectral boundary element formulation, to calculate the hydraulic permeability of ordered, three dimensional fibrous media. In [28], the tensor of permeability of the fibrous porous media is determined based upon a generalized cell model proposed by Neale et al. [35]. For three dimensional disordered fibrous media we cite for example [14, 22].

In this work, we are concerned with studying the flow through a realistic class of fibrous media using homogenization techniques. In section 2, we give a description of the locally quasi-periodic fibrous medium, consisting of layers of parallel fibers. This particular fibre geometry corresponds to a description of a biological tissue and was first studied by M. Briane. We note that our approach applies to other geometries studied in the papers of Briane from 1993-94. Next, we present our model problem (Stokes problem) and we homogenize it, using a two-scale expansion. We derive the effective Darcy equation and the permeability. The formal result, which differs significantly from the standard derivation of the Darcy law for a filtration through a periodic rigid porous medium, is rigorously justified in the Appendix. For computing the effective permeability tensor, we identify and solve a variational problem called the *cell problem*. For a practical calculation of the permeability tensor, we introduce and solve two generic cell problems described by a  $2D$  Stokes problem and a  $2D$  Poisson problem respectively. Consequently, we obtain a new formula of the permeability tensor which is function of the geometry of the above-mentioned generic cells. For the sake of illustration, we present an example of numerical results that show the influence of the orientation of the fibers in two cases: parallel fibers and variable orientations. Our goal in section 3 is to present a rigorous theoretical analysis consisting in determining formulae of the permeability in the low solid fraction limit. We show that the leading terms of our formulae are consistent with empirical formulae given in the literature. Also, we compare the predictions of asymptotic formulae with the results of numerical simulations. As already said, we address in the Appendix the technical question of the error made, when the physical velocity and the physical pressure are approximated by the homogenized quantities introduced in section 2.

Our conclusion is that the homogenization approach allows to calculate the permeability of fibrous media in a very efficient way. It also allows to confirm the validity, at the leading order of the low fraction limit, of the empirical formulas used in engineering. Let us note that the generalization to the determination of the dynamic permeability (see [1] and references therein for the definition) of fibrous media is straightforward.

## 2 Permeability of a fibrous medium

### 2.1 Notations and geometry definition

One of the rare mathematical references on fibrous porous media is the work by M. Briane. He considered homogenization of an elliptic 2nd order operator with oscillatory coefficients in such setting. More precisely, he studied the behavior of fibrous materials with respect to heat conduction. The conductivity matrix took different values in the fibres and in the interstitial medium.

The assumptions on the fiber geometry were motivated by biomechanical applications and Briane studied three cases. They all deal with tiny fibers, perpendicular to the  $x_1$ -axis and making locally an angle  $\gamma(x_1)$  with the  $x_2$ -axis.

His first model was a stratified periodic structure and its drawback was that fibers were not cylindrical. The drawback was rectified by the sophisticated third model, which is no more locally periodic. For more details we refer to Briane's papers [11, 12, 13]. The second model was, according to Briane (see his Ph. D. thesis [11], page 202) the closest to the biomechanical models used in applications. In this case, the fibrous material was locally periodic and its particularity was that the variations of the orientation function  $\gamma$  did not appear in the effective equation.

Motivated by its importance in the applications, we will deal with it.

To define the geometry of the porous medium, we follow the second case considered by M. Briane in [12] (see also [11, 13]). Let  $\Omega$  be a domain in  $\mathbb{R}^3$  which consists of  $N_\varepsilon$  layers, denoted by  $\Omega^{\varepsilon,n}$ ,  $n = 1, \dots, N_\varepsilon$ , perpendicular to the  $Ox_1$  axis. The thickness along  $Ox_1$  of each layer is  $\varepsilon^r$ , with  $0 < r < 1$ . Let  $x^{\varepsilon,n}$  be a given point in  $\Omega^{\varepsilon,n}$ , for  $n = 1, \dots, N_\varepsilon$ , and  $\gamma$  a  $\mathcal{C}^1(\mathbb{R})$  function. In the layer  $\Omega^{\varepsilon,n}$ , there are  $1/\varepsilon^{1-r}$  rows of fibers of radius  $\varepsilon R$  which constitute a periodic network of cylinders whose axes are parallel, perpendicular to  $Ox_1$ , and make an angle  $\gamma_{\varepsilon,n} = \gamma(x_1^{\varepsilon,n})$  with  $Ox_2$ . This angle is constant inside a layer, but changes from one layer to another. It is shown on Figure 1 a geometry with a function  $\gamma$  which varies linearly with the coordinate  $x_1$  of the layers. Figure 2 shows a magnified view of this configuration.

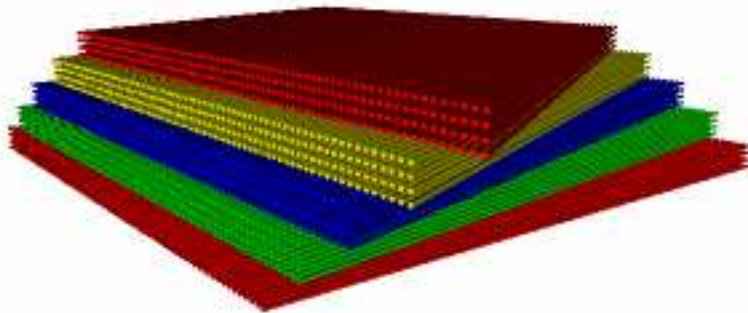


Figure 1: Microscopic geometry of the fibers (the vertical is  $Ox_1$ ).

To be more precise, let  $R \in (0, 1)$ ,  $\mathcal{Y} = [-1, 1] \times [-1, 1]$  and let  $\chi$  be the  $\mathcal{Y}$ -periodic function defined on  $\mathcal{Y}$  by:

$$\chi(y) = 1 \quad \text{if } |y| \leq R, \quad \text{and } \chi(y) = 0 \quad \text{if } |y| > R.$$



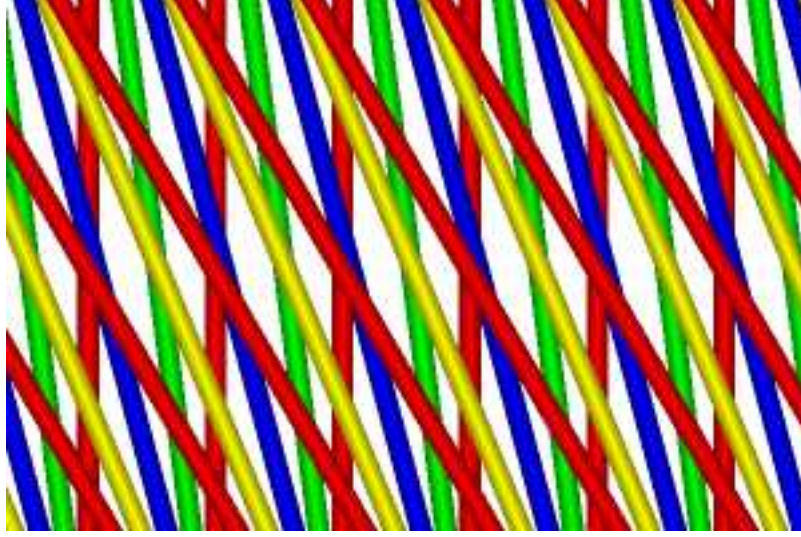


Figure 2: Microscopic geometry of the fibers (view along  $Ox_1$ ).

We denote by  $\mathcal{Y}_F$  the set  $\{y \in \mathcal{Y}, \chi(y) = 0\}$  and by  $\rho$  the function defined on  $\mathbb{R} \times \mathbb{R}^3$  with values in  $\mathbb{R}^2$ :

$$\rho(\zeta, x) = (x_1, x_3 \cos \gamma(\zeta) - x_2 \sin \gamma(\zeta))$$

with  $x = (x_1, x_2, x_3)$ . In the layer  $n$ , the fibrous domain is defined by

$$\Omega_s^{\varepsilon, n} = \left\{ x \in \Omega, \chi \left( \frac{\rho(x_1^{\varepsilon, n}, x)}{\varepsilon} \right) = 1 \right\},$$

and the fluid domain  $\Omega^{\varepsilon, n}$  by:

$$\Omega^{\varepsilon, n} = \Omega \setminus \Omega_s^{\varepsilon, n}.$$

We then defined  $\Omega^\varepsilon$  (resp.  $\Omega_s^\varepsilon$ ) as the union of all the layers  $\Omega^{\varepsilon, n}$  (resp.  $\Omega_s^{\varepsilon, n}$ ).

## 2.2 Homogenization

The flow in  $\Omega^\varepsilon$  is assumed to be governed by the Stokes equations:

$$-\nu \Delta \mathbf{u}^\varepsilon + \nabla p^\varepsilon = \mathbf{f} \quad \text{in } \Omega^\varepsilon, \quad (2)$$

$$\operatorname{div} \mathbf{u}^\varepsilon = 0 \quad \text{in } \Omega^\varepsilon, \quad (3)$$

$$\mathbf{u}^\varepsilon = 0 \quad \text{on } \partial\Omega^\varepsilon. \quad (4)$$

Each layer is homogenized independently, which is justified by the difference of scales of the fibers ( $\varepsilon$ ) and the layer ( $\varepsilon^r$ ). In order to homogenize the Stokes system (2)-(4) in  $\Omega^{\varepsilon,n}$ , the functions  $\mathbf{u}$  and  $p$  are supposed to have the following expansions (see [10]):

$$\mathbf{u}^\varepsilon(x) = \varepsilon^2 \mathbf{u}^0 \left( x, \frac{\rho(x_1^{\varepsilon,n}, x)}{\varepsilon} \right) + \dots \quad (5)$$

$$p^\varepsilon(x) = p^0 \left( x, \frac{\rho(x_1^{\varepsilon,n}, x)}{\varepsilon} \right) + \varepsilon p^1 \left( x, \frac{\rho(x_1^{\varepsilon,n}, x)}{\varepsilon} \right) + \dots \quad (6)$$

To perform the formal two-scale analysis, it is convenient to introduce a mapping  $\varphi_{\varepsilon,n}$  from a reference configuration  $\hat{\Omega}^{\varepsilon,n}$  onto  $\Omega^{\varepsilon,n}$ . We define  $\hat{u}$  in the reference configuration by  $\hat{u}(\hat{x}_1, \hat{x}_2, \hat{x}_3) = u(x_1, x_2, x_3)$ , with  $(x_1, x_2, x_3) = \varphi_{\varepsilon,n}(\hat{x}_1, \hat{x}_2, \hat{x}_3)$ . The functions  $\hat{p}$  and  $\hat{\mathbf{f}}$  are defined accordingly. The deformation gradient is given by

$$\mathbf{F} = \left[ \frac{\partial x_i}{\partial \hat{x}_j} \right]_{i,j=1,2,3}.$$

The determinant of  $\mathbf{F}$  is denoted by  $J$  and  $\mathbf{F}^{-1}$  is denoted by  $\mathbf{G}$ . Using the following identities:  $\nabla p = \mathbf{G}^T \nabla_{\hat{x}} \hat{p}$ ,  $\nabla \mathbf{u} = \nabla_{\hat{x}} \hat{\mathbf{u}} \mathbf{G}$ ,  $\operatorname{div}_{\hat{x}} (J \nabla_{\hat{x}} \hat{\mathbf{u}} \mathbf{G} \mathbf{G}^T) = J \operatorname{div}(\nabla \mathbf{u})$  and  $\operatorname{div}_{\hat{x}} (J \mathbf{G}^T) = 0$ , we obtain:

$$-\nu \operatorname{div}_{\hat{x}} (J \nabla_{\hat{x}} \hat{\mathbf{u}}^\varepsilon \mathbf{G} \mathbf{G}^T) + \operatorname{div}_{\hat{x}} (J \hat{p}^\varepsilon \mathbf{G}^T) = J \hat{\mathbf{f}} \quad \text{in } \hat{\Omega}^{\varepsilon,n}, \quad (7)$$

$$\operatorname{div}_{\hat{x}} (J \mathbf{G} \hat{\mathbf{u}}^\varepsilon) = 0 \quad \text{in } \hat{\Omega}^{\varepsilon,n}, \quad (8)$$

$$\hat{\mathbf{u}}^\varepsilon = 0 \quad \text{on } \partial \hat{\Omega}^{\varepsilon,n}. \quad (9)$$

We note that for a matrix valued function  $A$ ,  $(\operatorname{div} A)_i = \sum_j \frac{\partial A_{ij}}{\partial x_j}$ . Thus, denoting by  $g_{ij}$  the components of  $\mathbf{G}$  and by  $h_{ij}$  the components of  $\mathbf{G} \mathbf{G}^T$ , we have for  $i = 1, 2, 3$ :

$$-\nu \sum_{j=1}^3 \frac{\partial}{\partial \hat{x}_j} \left[ J \sum_{k=1}^3 \frac{\partial \hat{u}_i}{\partial \hat{x}_k} h_{kj} \right] + \sum_{j=1}^3 \frac{\partial (J g_{ji} \hat{p}^\varepsilon)}{\partial \hat{x}_j} = J \hat{f}_i \quad \text{in } \hat{\Omega}^{\varepsilon,n}, \quad (10)$$

$$\sum_{i,j=1}^3 \frac{\partial (J g_{ji} \hat{u}_i)}{\partial \hat{x}_j} = 0 \quad \text{in } \hat{\Omega}^{\varepsilon,n}, \quad (11)$$

$$u_i^\varepsilon = 0 \quad \text{on } \partial \hat{\Omega}^{\varepsilon,n}. \quad (12)$$

In the reference configuration  $\hat{\Omega}^{\varepsilon,n}$ , the functions  $\hat{\mathbf{u}}$  and  $\hat{p}$  have the following expansions

$$\hat{\mathbf{u}}^\varepsilon(\hat{x}) = \varepsilon^2 \hat{\mathbf{u}}^0 \left( \hat{x}, \frac{\hat{x}_1}{\varepsilon}, \frac{\hat{x}_2}{\varepsilon} \right) + \dots \quad (13)$$

$$\hat{p}^\varepsilon(\hat{x}) = \hat{p}^0 \left( \hat{x}, \frac{\hat{x}_1}{\varepsilon}, \frac{\hat{x}_2}{\varepsilon} \right) + \varepsilon \hat{p}^1 \left( \hat{x}, \frac{\hat{x}_1}{\varepsilon}, \frac{\hat{x}_2}{\varepsilon} \right) + \dots \quad (14)$$

with  $\hat{x} = (\hat{x}_1, \hat{x}_2, \hat{x}_3)$ . We denote by  $\hat{z} = (\hat{z}_1, \hat{z}_2) = (\hat{x}_1/\varepsilon, \hat{x}_2/\varepsilon)$  the fine scale. First, putting these expressions into (10), we obtain with the  $O(1/\varepsilon)$  terms:

$$\frac{\partial}{\partial \hat{z}_1}(g_{1i}\hat{p}^0) + \frac{\partial}{\partial \hat{z}_2}(g_{2i}\hat{p}^0) = 0, \quad i = 1, 2, 3.$$

The matrix  $\mathbf{G}$  being regular, these relations yield  $\partial_{\hat{z}_1}\hat{p}^0 = \partial_{\hat{z}_2}\hat{p}^0 = 0$ , and thus

$$\hat{p}^0 = \hat{p}^0(\hat{x}). \quad (15)$$

Next, the  $O(1)$  terms in (10) and (11) give

$$\begin{aligned} & -\nu \frac{\partial}{\partial \hat{z}_1} [Jh_{11} \frac{\partial \hat{u}_i^0}{\partial \hat{z}_1} + Jh_{12} \frac{\partial \hat{u}_i^0}{\partial \hat{z}_2}] - \nu \frac{\partial}{\partial \hat{z}_2} [Jh_{21} \frac{\partial \hat{u}_i^0}{\partial \hat{z}_1} + Jh_{22} \frac{\partial \hat{u}_i^0}{\partial \hat{z}_2}] \\ & + \sum_{r=1}^2 \frac{\partial}{\partial \hat{z}_r} (Jg_{ri}\hat{p}^1) = Jf_i - \sum_{r=1}^3 \frac{\partial}{\partial \hat{x}_r} (Jg_{ri}\hat{p}^0) \end{aligned} \quad (16)$$

in  $\hat{\Omega}^{\varepsilon, n} \times \mathcal{Y}_F$ , for  $i = 1, 2, 3$ , and

$$\frac{\partial}{\partial \hat{z}_1} \left[ \sum_{i=1}^3 Jg_{1i}\hat{u}_i^0 \right] + \frac{\partial}{\partial \hat{z}_2} \left[ \sum_{i=1}^3 Jg_{2i}\hat{u}_i^0 \right] = 0 \quad (17)$$

in  $\hat{\Omega}^{\varepsilon, n} \times \mathcal{Y}_F$ . We have moreover

$$\hat{\mathbf{u}}^0(\hat{x}, \hat{z}_1, \hat{z}_2) = 0 \quad \text{on } \hat{\Omega}^\varepsilon \times \partial\mathcal{Y}_F \setminus \partial\mathcal{Y}, \quad (18)$$

$$(\hat{\mathbf{u}}^0, \hat{p}^1) \text{ is } \mathcal{Y}\text{-periodic in } (\hat{z}_1, \hat{z}_2), \quad (19)$$

$$\sum_{i,j=1}^3 g_{ji} \int_{\mathcal{Y}_F} \frac{\partial \hat{u}_i^0}{\partial \hat{x}_j}(\hat{x}, \hat{z}_1, \hat{z}_2) d\hat{z}_1 d\hat{z}_2 = 0 \quad \text{in } \hat{\Omega}^{\varepsilon, n}, \quad (20)$$

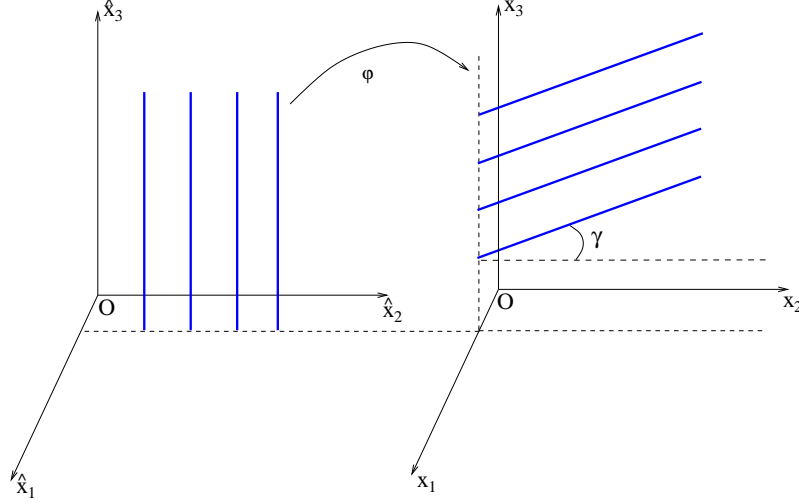
$$\int_{\partial\mathcal{Y}_F} \hat{\mathbf{u}}^0(\hat{x}, \hat{z}_1, \hat{z}_2) \cdot \mathbf{n} d\hat{z}_1 d\hat{z}_2 = 0 \quad \text{on } \partial\hat{\Omega}^{\varepsilon, n}. \quad (21)$$

For the mapping  $\varphi_{\varepsilon, n}$ , we choose a rotation that transforms fibers parallel to the  $O\hat{x}_3$  axis on the fibers of the layer  $\Omega^{\varepsilon, n}$  (see Fig. 3). More precisely:

$$(\hat{x}_1, \hat{x}_2, \hat{x}_3) = \varphi_{\varepsilon, n}^{-1}(x_1, x_2, x_3) = \begin{cases} x_1 \\ -x_2 \sin \gamma_{\varepsilon, n} + x_3 \cos \gamma_{\varepsilon, n} \\ -x_2 \cos \gamma_{\varepsilon, n} - x_3 \sin \gamma_{\varepsilon, n} \end{cases} \quad (22)$$

For this choice, we have

$$\mathbf{G} = \begin{bmatrix} 1 & 0 & 0 \\ 0 & -\sin \gamma_{\varepsilon, n} & \cos \gamma_{\varepsilon, n} \\ 0 & -\cos \gamma_{\varepsilon, n} & -\sin \gamma_{\varepsilon, n} \end{bmatrix}, \quad J = 1, \quad \mathbf{G}\mathbf{G}^T = Id$$

Figure 3: The mapping  $\varphi^{\epsilon, n}$ 

and equations (16) and (17) simply read:

$$\left\{ \begin{array}{l} -\nu \Delta_{\hat{z}_1, \hat{z}_2} \hat{u}_1^0 + \frac{\partial \hat{p}^1}{\partial \hat{z}_1} = \hat{f}_1 - \frac{\partial \hat{p}^0}{\partial \hat{x}_1} \\ -\nu \Delta_{\hat{z}_1, \hat{z}_2} \hat{u}_2^0 - \sin \gamma_{\epsilon, n} \frac{\partial \hat{p}^1}{\partial \hat{z}_2} = \hat{f}_2 - \sin \gamma_{\epsilon, n} \frac{\partial \hat{p}^0}{\partial \hat{x}_2} - \cos \gamma_{\epsilon, n} \frac{\partial \hat{p}^0}{\partial \hat{x}_3} \\ -\nu \Delta_{\hat{z}_1, \hat{z}_2} \hat{u}_3^0 + \cos \gamma_{\epsilon, n} \frac{\partial \hat{p}^1}{\partial \hat{z}_2} = \hat{f}_3 + \cos \gamma_{\epsilon, n} \frac{\partial \hat{p}^0}{\partial \hat{x}_2} - \sin \gamma_{\epsilon, n} \frac{\partial \hat{p}^0}{\partial \hat{x}_3} \\ \frac{\partial \hat{u}_1^0}{\partial \hat{z}_1} + \frac{\partial}{\partial \hat{z}_2} \left( -\hat{u}_2^0 \sin \gamma_{\epsilon, n} + \hat{u}_3^0 \cos \gamma_{\epsilon, n} \right) = 0. \end{array} \right. \quad (23)$$

The scales cannot be separated in this system. Nevertheless, taking advantage of the fact that the right-hand side does not depend on  $\hat{z}$ , we can obtain the solution by solving the following “cell” problem: Let  $\{\omega^j, \pi^j\}$ ,  $j = 1, 2, 3$  the functions defined as the solutions to:

$$\left\{ \begin{array}{l} -\Delta_{\hat{z}_1, \hat{z}_2} \omega_1^j(x_1, \hat{z}_1, \hat{z}_2) + \partial_{\hat{z}_1} \pi^j = \delta_{1j} \quad \text{in } \mathcal{Y}_F, \\ -\Delta_{\hat{z}_1, \hat{z}_2} \omega_2^j(x_1, \hat{z}_1, \hat{z}_2) - \sin \gamma(x_1) \partial_{\hat{z}_2} \pi^j = \delta_{2j} \quad \text{in } \mathcal{Y}_F, \\ -\Delta_{\hat{z}_1, \hat{z}_2} \omega_3^j(x_1, \hat{z}_1, \hat{z}_2) + \cos \gamma(x_1) \partial_{\hat{z}_2} \pi^j = \delta_{3j} \quad \text{in } \mathcal{Y}_F, \\ \partial_{\hat{z}_1} \omega_1^j + \partial_{\hat{z}_2} (-\sin \gamma(x_1) \omega_2^j + \cos \gamma(x_1) \omega_3^j) = 0 \quad \text{in } \mathcal{Y}_F, \\ \omega^j(x_1, \hat{z}_1, \hat{z}_2) = 0 \quad \text{on } \partial \mathcal{Y}_F \setminus \partial \mathcal{Y}, \\ \{\omega^j, \pi^j\} \text{ is } \mathcal{Y}\text{-periodic in } (\hat{z}_1, \hat{z}_2). \end{array} \right. \quad (24)$$

**Proposition 1**

1. Problem (24) admits a unique solution  $(\omega^j, \pi^j) \in H^1(\mathcal{Y}_F)^3 \times L^2(\mathcal{Y}_F)$ .
2. The function  $\mathbf{u}^0$  in (5) is given by

$$\mathbf{u}^0(x, z_1, z_2) = \frac{1}{\nu} \sum_{j=1}^3 \left( f_j(x) - \frac{\partial p^0}{\partial x_j}(x) \right) \omega^j(x_1, z_1, z_2) \quad (25)$$

3. The effective pressure  $p^0$  in (6) only depends on  $x$  and is solution to the Darcy problem:

$$\begin{cases} \mathbf{u}^D(x) &= \frac{\mathbf{K}(x_1)}{\nu} (\mathbf{f} - \nabla p^0(x)) & \text{in } \Omega, \\ \operatorname{div} \mathbf{u}^D &= 0, & \text{in } \Omega, \\ \mathbf{u}^D \cdot \mathbf{n} &= 0, & \text{on } \partial\Omega. \end{cases} \quad (26)$$

where the permeability matrix  $\mathbf{K} = [K_{i,j}]_{i,j=1,2,3}$  is given by

$$K_{ij}(x_1) = \frac{1}{|\mathcal{Y}|} \int_{\mathcal{Y}_F} \omega_i^j(x_1, z_1, z_2) dz_1 dz_2. \quad (27)$$

Note that formula (27) is not convenient from the numerical viewpoint since it depends on the macroscopic variable  $x_1$ . A more practical formula involving cell problems independent of  $x_1$  will be given in section 2.3.

**Proof.**

1. The analysis of (24) is rather straightforward. We postpone it until section 2.3 where a constructive proof is given (see Remark 2.1).

2. The fact that  $p^0$  does not depend on the fine scale has been established above (see (15)). Next, we multiply equations (24) by  $\frac{1}{\nu} \left( \hat{f}_j(\hat{x}) - (\mathbf{G}^T \nabla_{\hat{x}} \hat{p}^0)_j \right)$ , for  $j = 1, 2, 3$ . Then, summing these equations, we obtain that  $(\hat{u}_1^0, \hat{u}_2^0, \hat{u}_3^0, \hat{p}^1)$  defined by

$$\hat{u}_i^0 = \sum_{j=1}^3 \frac{1}{\nu} \left( \hat{f}_j - (\mathbf{G}^T \nabla_{\hat{x}} \hat{p}^0)_j \right) \omega_i^j$$

and

$$\hat{p}^1 = \sum_{j=1}^3 \left( \hat{f}_j - (\mathbf{G}^T \nabla_{\hat{x}} \hat{p}^0)_j \right) \pi^j$$

is solution to (23). Thus using the relation  $\nabla p^0 = \mathbf{G}^T \nabla_{\hat{x}} \hat{p}^0$ , we obtain (25).

3. Defining the Darcy velocity by:

$$\mathbf{u}^D(x) = \frac{1}{|\mathcal{Y}|} \int_{\mathcal{Y}_F} \mathbf{u}^0(x, z_1, z_2) dz_1 dz_2$$

we straightforwardly obtain (26) with the definition (27) of the permeability tensor.  $\diamond$

The rigorous justification of the approximation is quite technical, but follows the general ideas used in the homogenization of the Stokes system in a porous medium and in the study of the interface conditions between two different porous media. We address it in some details in the Appendix. In fact we will not only prove that our filtration velocity and the effective pressure are the limits of the rescaled physical velocities and pressures, but we will also give an error estimate in terms of  $\varepsilon$ .

### 2.3 Cell problems

In order to address the effective computation of the permeability, we introduce the following generic cell problems: let  $U_1^j(z_1, z_2)$ ,  $U_2^j(z_1, z_2)$ ,  $P^j(z_1, z_2)$ ,  $j = 1, 2$  be the functions defined as the solutions to the 2D Stokes problems:

$$\left\{ \begin{array}{l} -\Delta_{z_1, z_2} U_1^j + \partial_{z_1} P^j = \delta_{1j} \quad \text{in } \mathcal{Y}_F, \\ -\Delta_{z_1, z_2} U_2^j + \partial_{z_2} P^j = \delta_{2j} \quad \text{in } \mathcal{Y}_F, \\ \partial_{z_1} U_1^j + \partial_{z_2} U_2^j = 0 \quad \text{in } \mathcal{Y}_F, \\ U_1^j = U_2^j = 0 \quad \text{on } \partial\mathcal{Y}_F \setminus \partial\mathcal{Y}, \\ \{U_1^j, U_2^j, P^j\} \text{ is } \mathcal{Y}\text{-periodic in } z_1, z_2, \end{array} \right. \quad (28)$$

and let  $V(z_1, z_2)$  be the solution to the 2D Poisson problem:

$$\left\{ \begin{array}{l} -\Delta V = 1 \quad \text{in } \mathcal{Y}_F, \\ V = 0 \quad \text{on } \partial\mathcal{Y}_F \setminus \partial\mathcal{Y}, \\ V \text{ is } \mathcal{Y}\text{-periodic in } z_1, z_2. \end{array} \right. \quad (29)$$

We introduce  $\tilde{\Omega}(x_1, z_1, z_2) = [\tilde{\omega}_i^j]_{i,j=1,2,3}$  defined by

$$\tilde{\Omega}(x_1, z_1, z_2) = \mathbf{R}^{-1}(x_1) \Omega(x_1, z_1, z_2),$$

with  $\Omega(x_1, z_1, z_2) = [\omega_i^j]_{i,j=1,2,3}$  and

$$\mathbf{R}(x_1) = \begin{bmatrix} 1 & 0 & 0 \\ 0 & \cos \gamma(x_1) & -\sin \gamma(x_1) \\ 0 & \sin \gamma(x_1) & \cos \gamma(x_1) \end{bmatrix}.$$

Combining the equations of system (28) and (29) we obtain:

$$\tilde{\Omega}(x_1, z_1, z_2) = \begin{bmatrix} U_1^1(z_1, z_2) & 0 & U_1^2(z_1, z_2) \\ 0 & V(z_1, z_2) & 0 \\ U_2^1(z_1, z_2) & 0 & U_2^2(z_1, z_2) \end{bmatrix} \mathbf{R}^{-1}(x_1).$$

From which we finally deduce

$$\mathbf{K}(x_1) = \mathbf{R}(x_1) \mathbf{K}_0 \mathbf{R}^{-1}(x_1) \quad (30)$$

with

$$\mathbf{K}_0 = \frac{1}{|\mathcal{Y}|} \begin{bmatrix} \int_{\mathcal{Y}_F} U_1^1 & 0 & \int_{\mathcal{Y}_F} U_1^2 \\ 0 & \int_{\mathcal{Y}_F} V & 0 \\ \int_{\mathcal{Y}_F} U_2^1 & 0 & \int_{\mathcal{Y}_F} U_2^2 \end{bmatrix}. \quad (31)$$

The developed expression for the permeability is given by

$$\mathbf{K}(x_1) = \begin{pmatrix} \overline{K}_{11} & -\overline{K}_{12}s & \overline{K}_{12}c \\ -\overline{K}_{21}s & \overline{K}_{22}s^2 + \overline{V}c^2 & (\overline{V} - \overline{K}_{22})cs \\ \overline{K}_{21}c & (\overline{V} - \overline{K}_{22})cs & \overline{V}s^2 + \overline{K}_{22}c^2 \end{pmatrix} \quad (32)$$

where the following notations have been used:  $c = \cos \gamma(x_1)$ ,  $s = \sin \gamma(x_1)$ ,

$$\overline{V} = \frac{1}{|\mathcal{Y}|} \int_{\mathcal{Y}_F} V \quad \text{and} \quad \overline{K}_{ij} = \frac{1}{|\mathcal{Y}|} \int_{\mathcal{Y}_F} U_j^i. \quad (33)$$

Consequently, once solved the three generic cell problems (28) with  $j=1,2$  and (29), the permeability is obtained at any macroscopic coordinate  $x_1$  by computing two simple matrix-matrix products (30).

For example, Figure 4 shows the velocity and pressure fields for the generic cell problem (28) with  $j = 1$ .

**Remark 2.1** Note that, the existence and uniqueness of  $(\mathbf{U}^j, P^j)$  and  $V$  being obvious, the relations

$$[\omega_i^j(x_1, z_1, z_2)] = R(x_1) \begin{bmatrix} U_1^1(z_1, z_2) & 0 & U_1^2(z_1, z_2) \\ 0 & V(z_1, z_2) & 0 \\ U_2^1(z_1, z_2) & 0 & U_2^2(z_1, z_2) \end{bmatrix} R^{-1}(x_1)$$

and

$$\pi^1 = P^1, \quad \pi^2 = -\sin \gamma P^2, \quad \pi^3 = \cos \gamma P^2$$

give a constructive proof of the existence and uniqueness of the solution to (24).

**Remark 2.2** Multiplying the first two equations of (28) by  $U_1^i$  and  $U_2^i$  respectively and integrating by parts, we obtain:

$$\int_{\mathcal{Y}_F} \nabla \mathbf{U}^i \cdot \nabla \mathbf{U}^j = \int_{\mathcal{Y}_F} \mathbf{U}^i \cdot \mathbf{e}_j.$$

Vectors  $\mathbf{U}^1$  and  $\mathbf{U}^2$  being independent, the matrix  $[\int_{\mathcal{Y}_F} \nabla \mathbf{U}^i \cdot \nabla \mathbf{U}^j]_{i,j=1,2}$  is invertible. In view of the definition of  $\mathbf{K}_0$  and relation (30), this implies that  $\mathbf{K}(x_1)$  is regular.

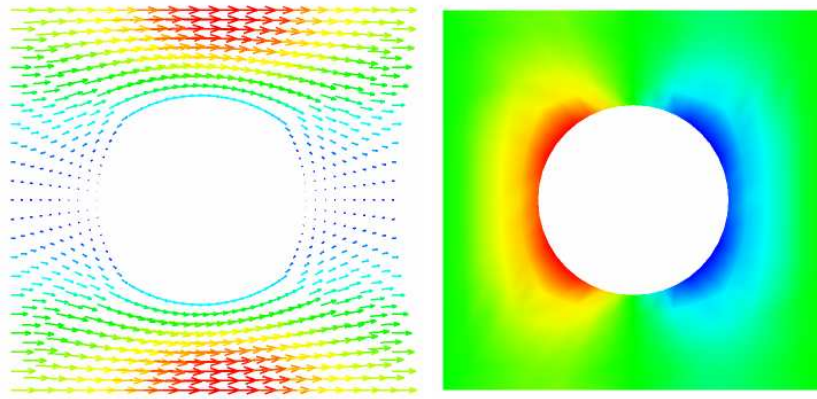


Figure 4: Velocity and pressure field for a cell problem



## 2.4 Numerical simulations

The numerical methods that we used to solve the various problems are reliable and standard, so we just sketch their description. The generic cell problems (28) are solved using Q2 finite element for the velocity and discontinuous P1 for the pressure. This pair of elements is known to satisfy the inf-sup condition ([17]), and is elementwise mass preserving. The Darcy equations (26) are also solved by mixed finite elements: the velocity is approximated in the lowest order 3D Raviart-Thomas finite element space (see for example [36]), and the pressure is constant by element. This choice ensures the continuity of the normal component of the velocity and an exact elementwise mass balance. Moreover, we adopt a mixed-hybrid formulation: a symmetric definite positive system is first solved by a preconditioned conjugate gradient method to compute the trace of the pressure on the faces on the elements; next the pressure and the velocity are recovered by a local procedure.

### 2.4.1 Parallel fibers: influence of the orientation

In this experiment, we impose a pressure drop between two opposite faces of a unit cube. The fibers are parallel and we investigate the influence of the angle between the fibers and the flow (which is mainly directed along  $Ox_2$ ). We report on Figure 5 the curves of the flux through a face of the cube *versus* the angle for three different sizes of the fibers. As expected, the flux is maximal (resp. minimal) for a flow parallel (resp. orthogonal) to the fibers, and is greater for smaller fibers.

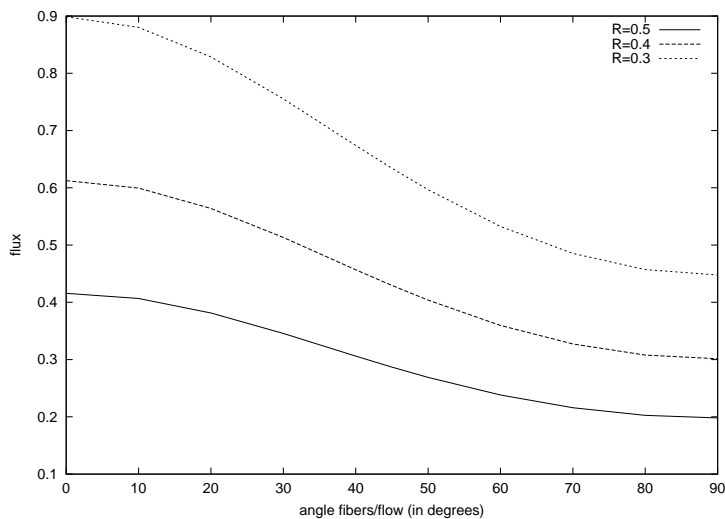


Figure 5: Influence of the angle between the fibers and the flow, and of the radius of the fibers.

### 2.4.2 An example with non-parallel fibers

In this experiment, we still impose a pressure drop between two opposite faces of a unit cube, but now the angle between the fibers and  $Ox_2$  is variable:  $\gamma(x_1) = 2\pi x_1$ . Figure 6 shows the influence of the orientation of the fibers on the velocity vectors.

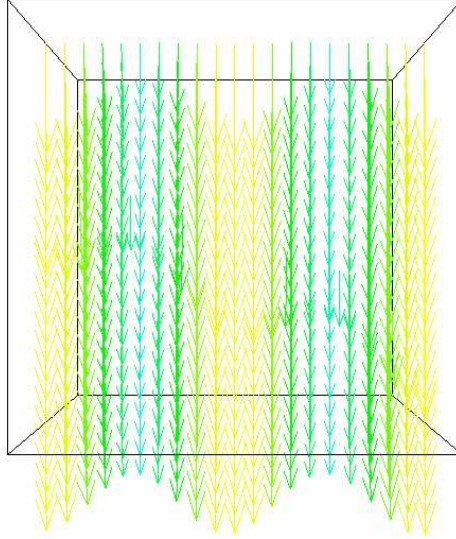


Figure 6: Velocity obtained with fibers making an angle  $\gamma(x_1) = 2\pi x_1$  with  $Ox_2$  (on this picture  $Ox_1$  is horizontal and  $Ox_2$  vertical).

## 3 Low solid fraction limit

In the applied literature (see *e.g.* [24] or [28] and references therein), the permeability in the low solid fraction limit is often assumed to be scalar and is searched of the form  $k = a^2 f(\varphi)$ , where  $a$  is the diameter of the fibers and  $\varphi$  the volume fraction of the solid material. More sophisticated models provide a homogeneous permeability tensor of the form

$$\mathbf{K} = \begin{pmatrix} K_{\perp} & 0 & 0 \\ 0 & K_{\parallel} & 0 \\ 0 & 0 & K_{\perp} \end{pmatrix} \quad (34)$$

where  $K_{\parallel}$  (resp.  $K_{\perp}$ ) corresponds to the permeability in the direction parallel (resp. orthogonal) to the fibers. The following expressions are derived in [18] in the case of fibers

with circular section:

$$K_{\parallel} = \frac{a^2}{4\varphi} \left( \log(1/\varphi) - 1.5 + 2\varphi - \frac{\varphi^2}{2} \right), \quad (35)$$

$$K_{\perp} = \frac{a^2}{8\varphi} \left( \log(1/\varphi) + \frac{\varphi^2 - 1}{\varphi^2 + 1} \right). \quad (36)$$

Many other expressions have been proposed in the literature and compared to experiments. Although they present slight differences, most of them share the same leading order terms. We refer to [24] and the references therein for a review of the most commonly used formulae and to [28] for some recent developments. In [30], these formulas were obtained by solving analytically approximated cell problems where periodicity were replaced by convenient boundary conditions.

Our expression for the permeability (32) with  $\gamma(x_1) = 0$  is:

$$\mathbf{K} = \begin{pmatrix} \overline{K}_{11} & 0 & \overline{K}_{12} \\ 0 & \overline{V} & 0 \\ \overline{K}_{21} & 0 & \overline{K}_{22} \end{pmatrix} \quad (37)$$

where  $\overline{K}_{ij}$  and  $\overline{V}$  are defined in (33). The purpose of this section is to compare this formula with (34). More precisely we shall compare  $K_{\parallel}$  with  $\overline{V}$  and

$$\begin{pmatrix} \overline{K}_{11} & \overline{K}_{12} \\ \overline{K}_{21} & \overline{K}_{22} \end{pmatrix} \quad \text{with} \quad \begin{pmatrix} K_{\perp} & 0 \\ 0 & K_{\perp} \end{pmatrix}.$$

In section 3.1, it is shown that the leading terms of our formulae are consistent with (35) and (36). In section 3.2, we compare the predictions of the asymptotic formulae with the results of numerical simulations of the model proposed in section 2.

### 3.1 Rigorous determination of the leading order terms

It has been seen in section 2, that the computation of the permeability tensor requires the solution of the auxiliary 2D Stokes problems

$$-\Delta_z \mathbf{U}^j + \nabla_z P^j = \mathbf{e}_j \quad \text{in } \mathcal{Y}_F \quad (38)$$

$$\operatorname{div}_z \mathbf{U}^j = 0 \quad \text{in } \mathcal{Y}_F \quad (39)$$

$$\mathbf{U}^j = 0 \quad \text{on } \partial \mathcal{Y}_F \setminus \partial \mathcal{Y} \quad (40)$$

$$\{\mathbf{U}^j, P^j\} \quad \text{is } \mathcal{Y} \text{ - periodic} \quad (41)$$

and the auxiliary 2D Poisson problem

$$-\Delta_z V = 1 \quad \text{in } \mathcal{Y}_F \quad (42)$$

$$V = 0 \quad \text{on } \partial \mathcal{Y}_F \setminus \partial \mathcal{Y} \quad (43)$$

$$V \quad \text{is } \mathcal{Y} \text{ - periodic} \quad (44)$$

Let us now suppose that the size of  $B = \mathcal{Y} \setminus \mathcal{Y}_F$  is of order  $\eta$ , *i.e.* that  $B = \eta B_0$  where the radius of  $B_0$  is of order 1. We would like to know what happens with the averages of  $\mathbf{U}^j$  and  $V$  when  $\eta \rightarrow 0+$ . This is the low solid fraction limit. We assume that  $\eta$  and  $\varepsilon$  go to zero in such a way that

$$\eta \gg \frac{1}{\varepsilon} e^{-1/\varepsilon^2}, \quad (45)$$

so that at the limit the effective flow is described by the Darcy law. For smaller obstacles, different limit regimes occur (Brinkman or Stokes equations).

Following [5], where this problem was studied rigorously, we set

$$-\Delta_z w^k + \nabla_z q^k = 0 \quad \text{in } \mathbb{R}^2 \setminus B_0 \quad (46)$$

$$\operatorname{div}_z w^k = 0 \quad \text{in } \mathbb{R}^2 \setminus B_0 \quad (47)$$

$$w^k = 0 \quad \text{on } \partial B_0 \quad (48)$$

$$w^k = (\log r) e_k \quad \text{in infinity, } r = |z|. \quad (49)$$

Then (46)-(49) has a unique solution being the sum of the special solution for the case of the unit circle and of the solution for a "difference" problem, where the velocity has a logarithmic asymptotic behavior at infinity. For details we refer to [6], [3], [4] and [5]. The asymptotic behavior is given by the following result:

**Proposition 2 ([5])**

We have

$$\{P^j(\eta y), \mathbf{U}^j(\eta y)\} \rightharpoonup \frac{1}{\pi} \{q^j(y), w^j(y)\} \quad (50)$$

weakly in  $L^2_{loc}(\mathbb{R}^2 \setminus B_0)/\mathbb{R} \times H^1_{loc}(\mathbb{R}^2 \setminus B_0)^2$ . Furthermore

$$\lim_{\eta \rightarrow 0} \frac{1}{|\log \eta| |\mathcal{Y}|} \int_{\mathcal{Y}_F} U_k^j dy = \frac{\delta_{jk}}{\pi}. \quad (51)$$

This result shows that the  $2 \times 2$  matrix  $(\overline{K}_{ij})$  is asymptotically a scalar matrix, confirming the observations from [18, 24, 28]. It also shows that

$$\overline{K}_{11} = \overline{K}_{22} \approx \frac{1}{\pi} |\log \eta|.$$

Formula (36) is therefore consistent with our result at the leading order with  $a = \eta$  and  $\varphi = \pi \eta^2 / 4$  ( $\pi \eta^2$  is the solid surface in the cell and 4 is the cell surface  $[-1, 1]^2$ ).

We now discuss the low solid fraction limit for  $V$ . A detailed mathematical article on the computation of dispersive media is [29]. It concentrates mainly on the Neumann boundary conditions. In such a case, simple asymptotic formulas of Rayleigh type have a high accuracy. In the case of Dirichlet boundary conditions, this kind of asymptotic formulas

is unfortunately much less accurate. The case of low solid fraction for the Dirichlet problem in a perforated domain has been addressed in [27] but only in 3D. In 2D we establish the following result.

**Proposition 3**

We have

$$V(\eta y) \rightharpoonup \frac{2v}{\pi} \quad \text{weakly in } H_{loc}^1(\mathbb{R}^2 \setminus B_0) \quad (52)$$

where  $v$  is the unique solution for the problem

$$-\Delta v = 0 \quad \text{in } \mathbb{R}^2 \setminus B_0 \quad (53)$$

$$v = 0 \quad \text{on } \partial B_0 \quad (54)$$

$$v = \log r \quad \text{at infinity, } r = |y|. \quad (55)$$

Furthermore

$$\lim_{\eta \rightarrow 0} \frac{1}{|\log \eta| |\mathcal{Y}|} \int_{\mathcal{Y}_F} V(y) dy = \frac{2}{\pi}. \quad (56)$$

**Proof.** It is a simplified version of the corresponding result for the Stokes system in [5] and we give only an outline.

First we introduce the sequence  $V^{0,\eta}$  defined by

$$\begin{cases} V^{0,\eta} = 0 & \text{in } B_1 \\ V^{0,\eta} = \frac{2}{\pi} \log r & \text{in } B_{1/\eta} \setminus B_1 \\ V^{0,\eta} = -\frac{2}{\pi} \log \eta & \text{in } \mathbb{R}^2 \setminus B_{1/\eta} \end{cases} \quad (57)$$

where  $B_{1/\eta}$  is the ball of radius  $1/\eta$  and  $V^{1,\eta}(x) = V(\eta x) - V^{0,\eta}(x)$ . Then it is easy to see that  $\nabla V^{1,\eta}$  is uniformly bounded in  $L^2(\eta^{-1}\mathcal{Y} \setminus B_0)$  and pass to the limit  $\eta \rightarrow 0$ . As in [5], we establish the a priori estimate in  $L^2$  with the weight  $(r+1)\log(r+2)$  for  $V^{1,\eta}$ . It leads to the conclusion that (52) holds true.

Next we have

$$\frac{1}{|\mathcal{Y}|} \int_{\mathcal{Y}_F} V(y) dy = \frac{2}{\pi} \log \frac{1}{\eta} + O(|\log \frac{1}{\eta}|^{1/2}) \quad (58)$$

where  $V^\eta(x) = V(\eta x)$  and the proposition is proved.  $\diamond$

The above result shows that the leading term in  $\bar{V}$  is  $\frac{2}{\pi} |\log \eta|$  which shows that our result is asymptotically consistent with formula (35) (taking as before  $a = \eta$  and  $\varphi = \eta^2 \pi/4$ ).

### 3.2 Numerical results

In order to assess the previous results, the cell problems (38)-(41) and (42)-(44) have been numerically solved for fibers with circular sections, with a solid fraction ranging from 0.2 to 0.002. Equations (35) and (36) have been plotted with  $a = \eta$  (the radius of the inclusion) and  $\varphi = \pi\eta^2/4$ . The agreement of  $\overline{K}_{ii}$  with formula (36) is reasonable and both curves have the same asymptotic behavior (Fig. 7, left). The agreement of  $\overline{V}$  with formula (35) is excellent on the whole range of solid fraction (Fig. 7, right).

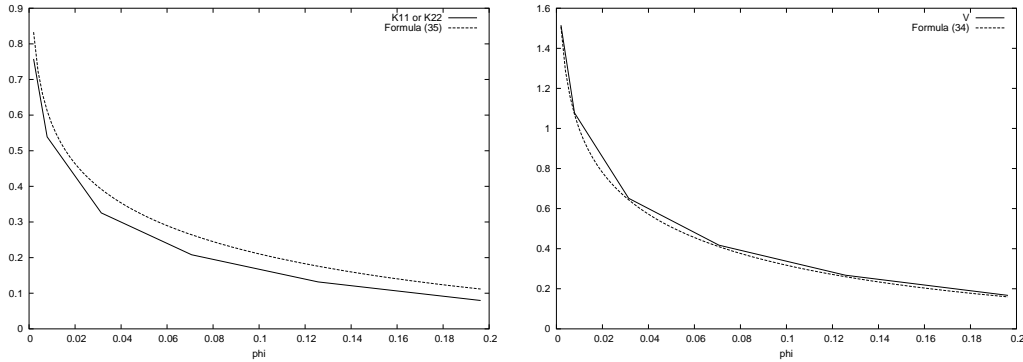


Figure 7: Fibers with a circular section. Left: comparison between  $\overline{K}_{ii}$  and Formula (36). Right: comparison between  $\overline{V}$  and Formula (35).

$\varphi$	$\overline{V}$	$\overline{K}_{ii}$
0.196299	0.167123	0.079633
0.125631	0.267833	0.131824
0.070667	0.417707	0.208051
0.031407	0.651478	0.325558
0.007851	1.077900	0.538937
0.001962	1.515430	0.757714

Table 1: Numerical values corresponding to Figure 7.

All the previous computations have been done with *circular* section fibers. An interesting property given by Propositions 2 and 3 is that the leading term of the asymptotic behavior is independent of the shape of the solid inclusion. To illustrate this fact, we present on Fig. 8 the results given by (56) and (51) compared to numerical simulations with *square* section fibers. The good agreement is striking.

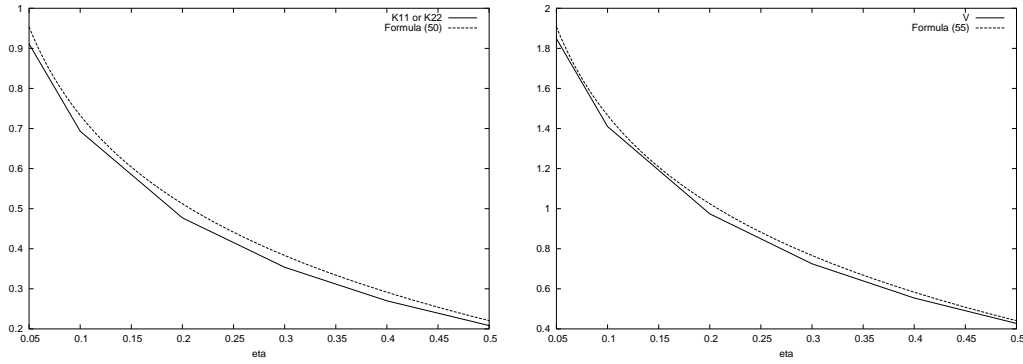


Figure 8: Fibers with a square section. Left: comparison between  $\overline{K}_{ii}$  and Formula (51). Right: comparison between  $\overline{V}$  and Formula (56).

$\eta$	$\overline{V}$	$\overline{K}_{ii}$
0.5	0.427491	0.208525
0.4	0.554049	0.270007
0.3	0.724945	0.353740
0.2	0.974281	0.477150
0.1	1.409805	0.693221
0.05	1.848851	0.911036

Table 2: Numerical values corresponding to Figure 8.

## Appendix

In this appendix we discuss the error made, when the physical velocity and the physical pressure are approximated by the homogenized quantities, introduced in section 2.

In the case of a periodic porous medium, the Darcy law was justified by L. Tartar in the late seventies. The proof that the Darcy velocity is the weak limit of  $\mathbf{u}^\varepsilon/\varepsilon^2$  is in [43]. For more details and generalizations to 3D geometries, one can consult the review chapter by G. Allaire in [7]. In fact, in the absence of external boundaries, it is possible to prove that  $\mathbf{u}^\varepsilon/\varepsilon^2 - \mathbf{u}^0$  and  $p^\varepsilon - p^0$  have  $L^2$ -norms of order  $\varepsilon$ . This confirms the formal asymptotic expansions. Nevertheless, the rigorous mathematical proof, which can be found in [34], requires also to correct the compressibility effects, coming from  $\mathbf{u}^\varepsilon$ . In fact, it is optimal to work in the Hilbert space, having finite  $L^2$ -norms of both the velocity field and its divergence.

Presence of outer boundaries complicates seriously the estimates. It was established in [33] that in the presence of an outer boundary, where physical velocity is zero,  $\mathbf{u}^0(x, x/\varepsilon)$  is a  $L^2$ -approximation of order  $\varepsilon^{1/(3m)}$ , where  $m = 2$  in the 2D case and  $m = 3$  in 3D. For Laplace operator, such an approximation is known to be of order  $\sqrt{\varepsilon}$ .

In our particular situation, we have also the interfaces. Namely,  $\mathbf{u}^0$  is constructed using (25) and it reads

$$\begin{aligned} \mathbf{u}^0(x, \frac{\rho(x_1^{\varepsilon,n}, x)}{\varepsilon}) &= \frac{1}{\nu} \sum_{j=1}^3 \left( f_j(x) - \frac{\partial p^0}{\partial x_j}(x) \right) \omega^j(x_1, z_1, z_2), \\ z_1 &= \frac{x_1}{\varepsilon}, \quad z_2 = \frac{x_3}{\varepsilon} \cos \gamma(x^{\varepsilon,n}) - \frac{x_2}{\varepsilon} \sin \gamma(x^{\varepsilon,n}) \end{aligned} \quad (59)$$

$$p^1(x, \frac{\rho(x_1^{\varepsilon,n}, x)}{\varepsilon}) = \sum_{j=1}^3 \left( f_j(x) - \frac{\partial p^0}{\partial x_j}(x) \right) \pi^j(x_1, z_1, z_2) \quad (60)$$

where  $\{\omega^j, \pi^j\}$  are defined by (24). Clearly, it depends on the parameter  $x^{\varepsilon,n}$ , saying in which layer we are.

Thus, inside every layer the differences

$$w_i^\varepsilon = \mathbf{u}_i^\varepsilon/\varepsilon^2 - \mathbf{u}_i^0(x, \frac{\rho(x_1^{\varepsilon,n}, x)}{\varepsilon}); \quad q^\varepsilon = p^\varepsilon - p^0(x) - \varepsilon p^1(x, \frac{\rho(x_1^{\varepsilon,n}, x)}{\varepsilon}) \quad (61)$$

satisfy the system

$$-\nu \varepsilon^2 \Delta w_i^\varepsilon + \frac{\partial}{\partial x_i} q^\varepsilon = -\Psi_i^\varepsilon \quad \text{in } \Omega^{\varepsilon,n}, i = 1, 2, 3, \quad (62)$$

$$\operatorname{div} w^\varepsilon = -\operatorname{div}_x \mathbf{u}^0(x, \frac{\rho(x_1^{\varepsilon,n}, x)}{\varepsilon}) \quad \text{in } \Omega^{\varepsilon,n} \quad (63)$$



with

$$\begin{aligned} \Psi_i^\varepsilon = & \varepsilon^2 J^{-1} \sum_{j=1}^3 \frac{\partial}{\partial \hat{x}_j} \left[ J \sum_{k=1}^3 \frac{\partial \hat{u}_i^0}{\partial \hat{x}_k} h_{kj} \right] + \varepsilon J^{-1} \left\{ \sum_{j=1}^3 \frac{\partial}{\partial \hat{x}_j} \left[ J \sum_{k=1}^2 \frac{\partial \hat{u}_i^0}{\partial \hat{z}_k} h_{kj} \right] + \right. \\ & \left. \sum_{j=1}^2 \frac{\partial}{\partial \hat{z}_j} \left[ J \sum_{k=1}^3 \frac{\partial \hat{u}_i^0}{\partial \hat{x}_k} h_{kj} \right] \right\} - \varepsilon J^{-1} \sum_{j=1}^3 \frac{\partial}{\partial \hat{x}_j} \left[ J g_{ji} p^1 \right]. \end{aligned} \quad (64)$$

After [34], we have

$$\left| \int_{\Omega^{\varepsilon,n}} \Psi^\varepsilon \varphi \, dx \right| \leq C \varepsilon^2 \|\nabla \varphi\|_{L^2(\Omega^{\varepsilon,n})} \quad (65)$$

for every  $\varphi \in H^1(\Omega^{\varepsilon,n})$ , being zero at the fibres boundaries.

Then one corrects the compressibility effects, by introducing the auxiliary problem

$$\mathcal{L}_{div} Q \equiv \frac{\partial Q_1}{\partial z_1} + \frac{\partial}{\partial z_2} \left( -\sin \gamma(x_1) Q_2 + \cos \gamma(x_1) Q_3 \right) = \operatorname{div}_{\hat{x}} (J G \hat{u}^0) \quad \text{in } \mathcal{Y}_F \quad (66)$$

$$Q \text{ is } \mathcal{Y} \text{-periodic in } (z_1, z_2). \quad (67)$$

Using the decomposition from section 2, we see that

$$\operatorname{div}_x \int_{\mathcal{Y}_F} \mathbf{u}^0(x, z_1, z_2) dz_1 dz_2 = \operatorname{div}_x \mathbf{u}^D = 0$$

is the necessary and sufficient condition for existence of at least one solution for (66)-(67). Clearly, there is no uniqueness and we can choose a smooth solution  $Q$  for (66)-(67).

Now, as in [34], we have

$$\begin{aligned} -\nu \varepsilon^2 \Delta \left( w_i^\varepsilon + \frac{\varepsilon}{\nu} Q(x, \frac{\rho(x_1^{\varepsilon,n}, x)}{\varepsilon}) \right) + \frac{\partial}{\partial x_i} q^\varepsilon = & -\Psi_i^\varepsilon - \frac{\varepsilon^3}{\nu} \Delta Q(x, \frac{\rho(x_1^{\varepsilon,n}, x)}{\varepsilon}) \\ \text{in } & \Omega^{\varepsilon,n}, \quad i = 1, 2, 3, \end{aligned} \quad (68)$$

$$\operatorname{div} \left( w^\varepsilon + \frac{\varepsilon}{\nu} Q(x, \frac{\rho(x_1^{\varepsilon,n}, x)}{\varepsilon}) \right) = \frac{\varepsilon}{\nu} \operatorname{div}_x Q(x, \frac{\rho(x_1^{\varepsilon,n}, x)}{\varepsilon}) \quad \text{in } \Omega^{\varepsilon,n}. \quad (69)$$

This means that  $\{w^\varepsilon + \frac{\varepsilon}{\nu} Q(x, \frac{\rho(x_1^{\varepsilon,n}, x)}{\varepsilon}), q^\varepsilon\}$  satisfies the Stokes system (68)-(69) with the force and the source terms of order  $\varepsilon^2$  in appropriate norms.

In the situation without external boundary one could proceed as in [34] and conclude that the  $L^2$ -norms of  $\{w^\varepsilon + \frac{\varepsilon}{\nu} Q(x, \frac{\rho(x_1^{\varepsilon,n}, x)}{\varepsilon})\}$  and  $q^\varepsilon$  are of order  $\varepsilon$ .

We are in presence of many layers  $\Omega^{\varepsilon,n}$  and the geometry differs from one layer to another. Consequently, the coefficients in problem (24) change with  $n$  and they depend on  $x^{\varepsilon,n}$ . Thus, there is a jump of  $\mathbf{u}^0$  at the interface between different layers. Furthermore, the layers are of size  $\varepsilon^r$  and this fact could also influence the estimates. By "gluing together" the layers, this difficulty will be avoided.

Homogenization of problems containing several different subdomains, is closely linked with the determination of the effective flow conditions at the interface between two different porous media. At mathematically rigorous level, these problems were considered by W. Jäger and A. Mikelić in a number of papers. The general theory of the corresponding boundary layers is in [25]. Our particular situation, with layers of fibres which should be glued together, has a lot of similarities with the determination of the transmission conditions at the interface between two porous media with different pore structures. The transmission conditions, involving continuity of the pressure and of the normal velocities, were rigorously established in the article [26]. We will follow the approach from [26].

Let us suppose that the interface between the layers  $\Omega^{\varepsilon,n}$  and  $\Omega^{\varepsilon,n+1}$  is at  $x_1 = c$ . Because of (22), the interface is stable under the mapping  $\varphi_{\varepsilon,n}$  and, following [26], we introduce the boundary layer problem which corrects the jump of  $\mathbf{u}^0$ . We denote by  $\mathcal{L}_S$  the Stokes operator corresponding to system (24). We denote the operator  $\mathcal{L}_S^+$  when the parameter in the coefficients is  $x^{\varepsilon,n+1}$ , and by  $\mathcal{L}_S^-$  otherwise (i.e. when the parameter is  $x^{\varepsilon,n}$ ). Analogously,  $\{\omega^{j,+}, \pi^{j,+}\}$  (resp.  $\{\omega^{j,-}, \pi^{j,-}\}$ ) is the solution for (24) for  $x = x^{\varepsilon,n+1}$  (resp. for  $x = x^{\varepsilon,n}$ ). Then the boundary layer problem reads

$$\mathcal{L}_S^+(\{\omega^{j,bl}, \pi^{j,bl}\}) = 0 \quad \text{in} \quad Z^+ = \cup_{k \in \mathbb{N} \cup \{0\}} (\mathcal{Y}_F + k\vec{e}_1) \quad (70)$$

$$\mathcal{L}_S^-(\{\omega^{j,bl}, \pi^{j,bl}\}) = 0 \quad \text{in} \quad Z^+ = \cup_{k \in \mathbb{N}} (\mathcal{Y}_F - k\vec{e}_1) \quad (71)$$

$$[\omega^{j,bl}] = \omega^{j,+} - K_{1j}(x^{\varepsilon,n+1})\vec{e}_1 - (\omega^{j,-} - K_{1j}(x^{\varepsilon,n})\vec{e}_1) \quad \text{at} \quad z_1 = 0 \quad (72)$$

$$\left[ \frac{\partial \omega_i^{j,bl}}{\partial z_1} - \pi^{j,bl} \delta_{1i} \right] = \frac{\partial \omega_i^{j,+}}{\partial z_1} - \pi^{j,+} \delta_{1i} - \left( \frac{\partial \omega_i^{j,-}}{\partial z_1} - \pi^{j,-} \delta_{1i} \right) \quad \text{at} \quad z_1 = 0 \quad (73)$$

$$\{\omega^{j,bl}, \pi^{j,bl}\} \quad \text{is periodic in} \quad z_2. \quad (74)$$

We note that the normal component of the jump  $[\omega^{j,bl}]$  at the interface  $x_1 = c$  has a zero mean.

Then by slightly generalizing the theory from [26], we get the solvability of problem (70)-(74) and the Saint-Venant principle saying that

$$|\nabla \omega^{j,bl}| + |\omega^{j,bl}| \leq c_0 e^{-c_1 |y_1|}, \quad \text{for some positive constants } c_0 \text{ and } c_1 \quad (75)$$

$$|\nabla \pi^{j,bl}| + |\pi^{j,bl} - H(z_1)C_1^j - H(-z_1)C_2^j| \leq c_0 e^{-c_1 |y_1|}. \quad (76)$$

Consequently, in the neighborhoods of the separating planes  $x_1 = c$  between two adjacent layers, our asymptotic expansion reads

$$\frac{\mathbf{u}^\varepsilon}{\varepsilon^2} = \mathbf{u}^0(x, \frac{\rho(x_1^{\varepsilon,n}, x)}{\varepsilon})H(c - x_1) + \mathbf{u}^0(x, \frac{\rho(x_1^{\varepsilon,n+1}, x)}{\varepsilon})H(x_1 - c) + \sum_{j=1}^3 \frac{\varepsilon}{\nu} (f_j - \frac{\partial p^0}{\partial x_j})(x) \omega^{j,bl} + (\text{compressibility corrections} + \text{higher order terms}) \quad (77)$$

$$p^\varepsilon = p^0(x) + \varepsilon p^1(x, \frac{\rho(x_1^{\varepsilon,n}, x)}{\varepsilon})H(c - x_1) + \varepsilon p^1(x, \frac{\rho(x_1^{\varepsilon,n+1}, x)}{\varepsilon})H(x_1 - c) + \sum_{j=1}^3 \frac{\varepsilon^2}{\nu} (f_j - \frac{\partial p^0}{\partial x_j})(x) \pi^{j,bl} + (\text{higher order terms}) \quad (78)$$

Let us check that the jump of  $\frac{\mathbf{u}^\varepsilon}{\varepsilon^2}$  at  $x_1 = c$  is zero.

First, in the tangential direction we have continuity of traces, by construction.

Next, in the normal direction we have

$$\frac{\mathbf{u}_1^\varepsilon}{\varepsilon^2} = \sum_{j=1}^3 (K_{1j}(x^{\varepsilon,n+1}) - K_{1j}(x^{\varepsilon,n})) f_j - \frac{\partial p^0}{\partial x_j} \Big|_{x_1=c} = 0, \quad (79)$$

since we imposed at the interfaces the continuity of  $K(f - \nabla p^0) \vec{e}_1$ , as the transmission condition. We note that it follows from those considerations that the continuity of the normal components of the filtration velocity is one of the necessary and sufficient conditions for having the correct order of approximation.

For this new approximation, we write an analogue of the system (68)-(69). Then, it is used for obtaining the estimate for the  $L^2$ -norm of the difference between  $\{\frac{\mathbf{u}^\varepsilon}{\varepsilon^2}, p^\varepsilon\}$  and the correction. Calculations are analogous to the ones from [26] and we have the following conclusions:

- a) The pressure is continuous at the layer interfaces. We note that the absolute value of the pressure jump is one of the leading terms in the error estimate and it should be set to zero in order to get an approximation. It is the second (and last) necessary and sufficient condition for obtaining the correct order of approximation. For detailed calculations we refer to [26].
- b)  $\omega^{j,bl}$  is of order  $c_0 \exp\{-c_1 \varepsilon^{r-1}\}$  at the other interfaces and we can simply ignore it there.
- c) Using that  $\rho \in C^1$ , we get that the boundary layer terms are of order  $\varepsilon^{r+3/2}$ . Since we have  $\varepsilon^{-r}$  boundary layers, this means a contribution of order  $\varepsilon^{3/2}$ .
- d) Keeping  $K(x^{\varepsilon,n})$  and  $K(x^{\varepsilon,n+1})$  deteriorates significantly the regularity of  $p^0$ . For this reason,  $K(x_1)$  should be used. This introduces an approximation error of order  $\varepsilon^r$ .

For small  $r$ , a possible solution is to take several intermediate values of  $x^{\varepsilon,n}$ . Attempts to work with less regular  $K$  lead to weaker error estimates and give raise to a global error of order  $\varepsilon^{1/8}$  (see [26]).

To conclude, in analogy with the results from [26], we have

**Theorem 1**

Let  $B_n$  be the  $n^{\text{th}}$  layer, containing fibres. Then we have

$$\left\| \frac{\mathbf{u}^\varepsilon}{\varepsilon^2} - \sum_{\text{over layers}} \chi_{B_n}(x) \frac{1}{\nu} \sum_{j=1}^3 \left( f_j(x) - \frac{\partial p^0}{\partial x_j}(x) \right) \omega^j \left( x_1, \frac{x_1}{\varepsilon}, \frac{x_3}{\varepsilon} \cos \gamma(x^{\varepsilon,n}) - \frac{x_2}{\varepsilon} \sin \gamma(x^{\varepsilon,n}) \right) \right\|_{L^2(\Omega)} \leq C \varepsilon^{\min\{1/6, r\}}, \quad (80)$$

$$\|p^\varepsilon - p^0\|_{L_0^2(\Omega)} \leq C \varepsilon^{\min\{1/6, r\}}. \quad (81)$$

With an appropriate choice of layers, the estimates (80)-(81) imply an interior estimate of order  $\sqrt{\varepsilon}$ .

**Acknowledgements:** The research of A.M. was supported by the GDR MOMAS (Modélisation Mathématique et Simulations numériques liées aux problèmes de gestion des déchets nucléaires: 2439 - ANDRA, BRGM, CEA, EDF, CNRS) as a part of the project "*Modélisation micro-macro des phénomènes couplés de transport-chimie-déformation en milieux argileux* "

## References

- [1] Y. Achdou and M. Avellaneda. Influence of pore roughness and pore-size dispersion in estimating the permeability of a porous medium from electrical measurements. *Phys. Fluids A.*, 4(12):2651–2673, 1992.
- [2] G. Allaire. Homogenization of the Stokes flow in a connected porous medium, *Asymptotic Analysis*, 2:203–222, 1989.
- [3] G. Allaire. Homogenization of the Navier-Stokes equations in open sets perforated with tiny holes. I. Abstract framework, a volume distribution of holes. *Arch. Rational Mech. Anal.*, 113(3):209–259, 1990.
- [4] G. Allaire. Homogenization of the Navier-Stokes equations in open sets perforated with tiny holes. II. Noncritical sizes of the holes for a volume distribution and a surface distribution of holes. *Arch. Rational Mech. Anal.*, 113(3):261–298, 1990.
- [5] G. Allaire. Continuity of the Darcy's law in the low-volume fraction limit. *Ann. Scuola Norm. Sup. Pisa Cl. Sci. (4)*, 18(4):475–499, 1991.

- 
- [6] G. Allaire. Homogenization of the Navier-Stokes equations with a slip boundary condition. *Comm. Pure Appl. Math.*, 44(6):605–641, 1991.
- [7] G. Allaire. One-Phase Newtonian Flow, in *Homogenization and Porous Media*, U. Hornung, ed., *Interdisciplinary Applied Mathematics Series*, Vol. 6, Springer, New York, 1997, pp. 45-68.
- [8] B. Bang and D. Lukkassen. Application of homogenization theory related to Stokes flow in porous media. *Appl. Math.*, 44(4):309–319, 1999.
- [9] A. Yu. Beliaev and S. M. Kozlov. Darcy equation for random porous media. *Comm. Pure Appl. Math.*, 49(1):1–34, 1996.
- [10] A. Bensoussan, J.-L. Lions, and G. Papanicolaou. *Asymptotic analysis for periodic structures*, volume 5 of *Studies in Mathematics and its Applications*. North-Holland Publishing Co., Amsterdam, 1978.
- [11] M. Briane. *Homogénéisation de matériaux fibrés et multi-couches*. PhD thesis, Université Paris VI, 1990.
- [12] M. Briane. Three models of nonperiodic fibrous materials obtained by homogenization. *RAIRO Modél. Math. Anal. Numér.*, 27(6):759–775, 1993.
- [13] M. Briane. Homogenization of a nonperiodic material. *J. Math. Pures Appl. (9)*, 73(1):47–66, 1994.
- [14] D. S. Clague and R. J. Phillips. A numerical calculation of the hydraulic permeability of the three-dimensional disordered fibrous media. *Phys. Fluid*, 9(6):1562–1572, 1997.
- [15] J. E. Drummond and M. I. Tahir. Laminar viscous flow through regular arrays of parallel solid cylinders. *Intl J. Multiphase Flow*, 10:515–540, 1984.
- [16] H.I. Ene and E. Sanchez-Palencia. Equations et phénomènes de surface pour l’écoulement dans un modèle de milieu poreux. *J. Mécan.*, 14:73–108, 1975.
- [17] V. Girault and P.-A. Raviart. *Finite element methods for Navier-Stokes equations*. Springer-Verlag, 1986.
- [18] J. Happel. Viscous flow relative to arrays of cylinders. *AIChE J.*, 5:174–177, 1959.
- [19] H. Hasimoto. On the periodic fundamental solutions of the Stokes equations and their application to viscous flow past a cubic array of spheres. *J. Fluid Mech.*, 5:174–177, 1959.
- [20] J. J. L. Higdon and G. D. Ford. Permeability of three-dimensional models of fibrous porous media. *J. Fluid Mech.*, 308:341–361, 1996.

- [21] I. D. Howells. Drag due to the motion of a Newtonian fluid through a sparse random array of small fixed rigid objects. *J. Fluid Mech.*, 64:449–475, 1974.
- [22] I. D. Howells. Drag on fixed beds of fibres in slow flow. *J. Fluid Mech.*, 355:163–192, 1998.
- [23] G.W. Jackson and D.F. James. The hydrodynamic resistance of hyaluronic acid and its contribution to tissue permeability. *Biorheology*, 19:317–330, 1982.
- [24] G.W. Jackson and D.F. James. The permeability of fibrous porous media. *The Canadian Journal of Chemical Engineering*, 64:364–374, 1986.
- [25] W. Jäger and A. Mikelić. On the boundary conditions at the contact interface between a porous medium and a free fluid, *Ann. Sc. Norm. Super. Pisa, Cl. Sci.- Ser. IV*, Vol. XXIII (1996), Fasc. 3, p. 403–465.
- [26] W. Jäger and A. Mikelić. On the boundary conditions at the contact interface between two porous media, in *Partial differential equations, Theory and numerical solution*, eds. W. Jäger, J. Nečas, O. John, K. Najzar, et J. Stará,  $\pi$  Chapman and Hall/CRC *Research Notes in Mathematics* n° 406, 1999. pp. 175–186.
- [27] V. V. Jikov, S. M. Kozlov, and O. A. Oleĭnik. *Homogenization of differential operators and integral functionals*. Springer-Verlag, Berlin, 1994.
- [28] J.A. Kolodziej, R. Dzięcielak, and Z. Kończak. Permeability tensor for heterogeneous porous medium of fibre type. *Transport in Porous Media*, 32:1–19, 1998.
- [29] S. Kozlov. Geometric aspects of homogenization. *Russian Math. Surveys*, 40:79–120, 1989.
- [30] S. Kuwabara. The force experienced by randomly distributed parallel circular cylinders or spheres in a viscous flow at small Reynolds number. *J. Phys. Soc. Japan*, 14:527–532, 1959.
- [31] R. E. Larson and J. J. L. Higdon. Microscopic flow near the surface of two-dimensional porous media. Part 1. Axial flow. *J. Fluid Mech.*, 166: 449–472, 1986.
- [32] R. E. Larson and J. J. L. Higdon. Microscopic flow near the surface of two-dimensional porous media. Part 2. Transverse flow. *J. Fluid Mech.*, 178: 119–136, 1987.
- [33] E. Marušić-Paloka and A. Mikelić. An error estimate for correctors in the homogenization of the Stokes and Navier-Stokes equations in a porous medium. *Boll. Unione Mat. Ital.*, (7) 10-A, n° 3, p. 661–671, 1996.
- [34] A. Mikelić. Homogenization theory and applications to filtration through porous media. In *Filtration in porous media and industrial application (Cetraro, 1998)*, volume 1734 of *Lecture Notes in Math.*, pages 127–214. Springer, Berlin, 2000.

- [35] G. Neale, H. Anaka and D. Hampel. Transport phenomena in non-homogeneous porous media. *Can. J. Chem. Eng.*, 53:691–694, 1975.
- [36] J. E. Roberts and J.-M. Thomas. *Handbook of numerical analysis*, volume Vol. II, chapter Mixed and hybrid methods, pages 523–639. North-Holland, 1991.
- [37] E. Sanchez-Palencia. Non-homogeneous media and vibrations theory. *Lecture Notes in Physics* 127, Springer-Verlag, Berlin, 1980.
- [38] A. S. Sangani and A. Acrivos. Slow flow past periodic arrays of cylinders with application to heat transfer. *Intl J. Multiphase Flow*, 8:193–206, 1982.
- [39] A. S. Sangani and C. Yao. Transport processes in random arrays of cylinders. I. Thermal conduction. *Phys. Fluids*, 31:2426–2434, 1988.
- [40] A. S. Sangani and C. Yao. Transport processes in random arrays of cylinders. II. Viscous flow. *Phys. Fluids*, 31:2435–2444, 1988.
- [41] E. M. Sparrow and A. L. Loeffler. Longitudinal laminar flow between cylinders arranged in a regular array. *AIChE J.*, 5:325–330, 1959.
- [42] L. Spielman and S. L. Goren. Model for predicting pressure drop and filtration efficiency in fibrous media. *Environ. Sci. Technol.*, 2:279–287, 1968.
- [43] L. Tartar. Convergence of the homogenization process, appendix in the book [37].



---

Unité de recherche INRIA Rocquencourt  
Domaine de Voluceau - Rocquencourt - BP 105 - 78153 Le Chesnay Cedex (France)

Unité de recherche INRIA Futurs : Parc Club Orsay Université - ZAC des Vignes  
4, rue Jacques Monod - 91893 ORSAY Cedex (France)

Unité de recherche INRIA Lorraine : LORIA, Technopôle de Nancy-Brabois - Campus scientifique  
615, rue du Jardin Botanique - BP 101 - 54602 Villers-lès-Nancy Cedex (France)

Unité de recherche INRIA Rennes : IRISA, Campus universitaire de Beaulieu - 35042 Rennes Cedex (France)

Unité de recherche INRIA Rhône-Alpes : 655, avenue de l'Europe - 38334 Montbonnot Saint-Ismier (France)

Unité de recherche INRIA Sophia Antipolis : 2004, route des Lucioles - BP 93 - 06902 Sophia Antipolis Cedex (France)

---

Éditeur  
INRIA - Domaine de Voluceau - Rocquencourt, BP 105 - 78153 Le Chesnay Cedex (France)  
<http://www.inria.fr>  
ISSN 0249-6399